ACS APPLIED MATERIALS & INTERFACES

Research Article

www.acsami.org

Shape Homogenization and Long-Range Arrangement of Gold Nanorods Using a pH-Responsive Multiamine Surfactant

Junwen Wu, Wenfeng Jia, Wensheng Lu,* and Long Jiang*

Beijing National Laboratory for Molecular Sciences, CAS Key Laboratory of Colloids and Surfaces, Institute of Chemistry, Chinese Academy of Sciences, Beijing 100190, People's Republic of China

Supporting Information

ABSTRACT: A relatively new and efficient method is reported here for the purification and arrangement of high-aspect-ratio gold nanorods (AuNRs) using a multiamine surfactant, bis[[(amidoethyl)carbamoyl]ethyl]octadecylamine (C18N3), which strongly adsorbs to the surface of AuNRs. The adsorbed layers of the multiamine surfactant on AuNRs exhibit the ability to deaggregate gold nanoparticles at low pH in an aqueous medium and to promote their aggregation at high pH. Through regulation of the pH of the dispersion medium, a well-ordered arrangement of 99% monodisperse AuNRs was obtained, having dimensions of approximately 18 nm diameter and 353 nm length and an area of several dozens of square micrometers, which is much larger than what has been reported in the literature. A very strong optical absorption in the near-infrared region of as-prepared AuNRs was shown. This strategy of using pH-responsive multiamine surfactant to mediate both the homogenization in shape and the arrangement of nanoparticles provides a new methodology for the formation of nanoparticle assemblies.

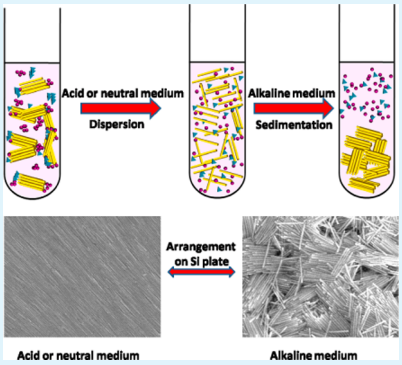

KEYWORDS: *nanorod, homogenization, arrangement, purifying, multiamine surfactant*

1. INTRODUCTION

Anisotropic gold nanoparticles (AuNPs) have been of great interest because their asymmetry often leads to novel physical and chemical properties.[1−8] All types of AuNPs, which have similar curvature, surface areas, and crystalline facets,[9] are prone to form distinct domains on a substrate; however, because of the similar settlement rates of differently shaped AuNPs, it is difficult to form a large domain consisting of AuNPs with a single morphology.[10−12] How to separate monodisperse, high-aspect-ratio gold nanorods (AuNRs) remains to be determined.[13] Recently, there have been reports of the successful separation of AuNRs by modifying the solution stability with salt or other methods to increase particle-shape-dependent discrimination,[14−16] but salt is difficult to remove despite several time-consuming rinses, thereby restricting its use. Centrifugation-assisted sedimentation is also adopted to purify these NIR-responsive AuNRs by taking advantage of the different shape-dependent sedimentation coefficients of the nanoparticles (NPs).[17] However, only a very low concentration of NP mixtures is applicable to this technology. Thus, a facile, low-cost process for this purpose is still needed.[18,19] In this study, we developed a new and efficient method for preparing and purifying monodisperse AuNRs from mixed AuNPs. By using a multiamine surfactant, bis[[(amidoethyl)carbamoyl]-ethyl]octadecylamine (C18N3),[20,21] which exhibited a much greater ability to not only replace cetyltrimethylammonium bromide on the crude AuNP surface via adsorption at low pH in an aqueous medium but also promote aggregation of AuNPs at high pH. As a result, 99% monodisperse AuNRs was obtained. Through the deposition of dispersions of as-purified AuNRs at low pH, a large-scale, well-ordered arrangement of AuNRs on a silicon substrate with an area of up to several dozens of square micrometers was obtained, which was much larger than has previously been reported. Arrangement of NPs has been studied intensively in the past few years[22] because of their possible future applications in the development of advanced optical, medical, and electrical nanodevices.[23−27]

2. EXPERIMENTAL SECTION

2.1. Chemicals. Cetyltrimethylammonium bromide (CTAB), nitric acid, $NaBH_4$, NaOH, chloroauric acid ($HAuCl_4{\cdot}4H_2O$), and ascorbic acid were purchased from the Beijing Chemical Reagent Plant, China. Bis[[(amidoethyl)carbamoyl]ethyl]octadecylamine (C18N3) was synthesized in a two-step process as described previously.[21] Deionized water was used throughout the experiments; all glassware was cleaned by aqua regia [HCl/HNO_3 in a 3:1 (v/v) ratio] and then rinsed with water prior to the experiments.

2.2. Synthesis of CTAB-Capped Gold Seeds for Growth of AuNRs. High-aspect-ratio AuNRs were synthesized by using a seed-mediated approach, as described by Wu et al.[28] In a typical experiment, CTAB-capped gold seeds were prepared by the addition of 0.6 mL of an ice-cold 10 mM $NaBH_4$ solution to 10 mL of 0.25 mM $HAuCl_4$, which was prepared in a 0.1 M CTAB solution, under vigorous stirring for 2 min. The yellow solution immediately changed to brown, indicating the formation of ultrasmall gold seeds. These seeds were

Received: August 14, 2012
Accepted: November 27, 2012
Published: November 27, 2012

then aged for 2 h to allow for the complete hydrolysis of unreached $NaBH_4$.

2.3. Preparation of the Growth Solution (GS) for AuNRs. An aqueous solution (100 mL) of 2.5×10^{-4} M $HAuCl_4$ was prepared, and then 1×10^{-2} mol of CTAB was added and stirred until completely dissolved.

2.4. Synthesis of AuNRs. Into flasks A and B, 0.1 M (25 μL) ascorbic acid was added to the GS (4.5 mL). Into flask C were added 0.1 M ascorbic acid (250 μL) and 0.1 M nitric acid (300 μL) to the GS (45 mL). The gold seed solution (400 μL) was subsequently added to the solution in flask A and stirred for 3 s. Then, the solution in flask A (400 μL) was immediately added to flask B and stirred for 5 s. Finally, 4 mL of the resulting solution in flask B was transferred to flask C and stirred for 5 s. The resulting solution in flask C was left undisturbed in a water bath at 26 ± 1 °C for 12 h until the reaction reached completion. The upper solution contained mostly spherical AuNPs and was removed; most of the high-aspect-ratio AuNRs settled to the bottom of the flask as precipitates. Finally, deionized water (5 mL) was added to redisperse the precipitates; the solution was brown.

2.5. Separation Procedures. To separate the AuNRs, the crude AuNR solution (5 mL) was centrifuged three times at 410*g* for 20 min to remove the extra surfactant molecules. This step was performed because highly concentrated CTAB (0.1 M) can crystallize at ambient temperature. Following centrifugation, the precipitates, which contained AuNRs and reaction byproducts, were dispersed in aqueous 1 mM C18N3 (1 mL). The total concentration of residual CTAB was minimal. A 1 M aqueous NaOH solution (5 μL) was added to this solution to adjust the pH from 8.3 to 11. The mixture was then kept at ambient temperature for 1 h without disturbance. Most of the AuNRs were deposited on the bottom of the beaker during the incubation period and were easily collected by removing the supernatant via pipetting. The AuNR precipitate was redispersed by ultrasonication to form a colloidal dispersion; the pH was adjusted with aqueous HCl for further characterization.

2.6. Arrangement Procedure. The AuNR precipitate was redispersed to form a colloidal dispersion by ultrasonication and adjustment of the pH by 1 M aqueous HCl from 8.5 to approximately 4 for AuNR arrangement.

2.7. Instrumentation. The morphologies of the AuNPs were characterized with a Hitachi S4800 scanning electron microscope with an accelerating voltage of 10.0 kV. The configuration of the products was characterized by a JEOL 1011 transmission electron microscope with an accelerating voltage of 100.0 kV. The UV−vis−near-infrared (NIR) absorption spectra of the AuNP solutions were recorded with a Hitachi U-4800 spectrometer. Background subtraction was performed for each spectrum using a wavelength range of 400−1100 nm and a 2-mm-path-length quartz cuvette to remove noise from the absorption of water in the NIR region. To obtain the absorption spectra of the AuNRs in the wavelength range of 1100−2500 nm, the concentrated NR precipitate, after rinsing using centrifugation, was transferred to quartz glass and air-dried. In contrast to the spectra in the 400−1100 nm range, the air was scanned for background subtraction instead of water. Solution-based size analyses were carried out at 26 °C and a scattering angle of 173° by a ZetaSizer Nano Series (Nano ZS, Malvern Instruments), which is equipped with a thermostat chamber and a 4 mW He−Ne laser (λ = 632.8 nm). For scanning electron microscopy (SEM) measurements, the suspension was placed on a silicon wafer and then dried in air.

3. RESULTS AND DISCUSSION

Purification and Homogenization of AuNRs by Changing the Surfactants at Different pH's. The method for preparing AuNRs originates from the method suggested by Wu et al., which is a modified seed-mediated synthesis approach based on the addition of an appropriate amount of nitric acid during nanorod growth.[28] Figure 1a shows freshly made AuNPs following several centrifugation steps to remove extra CTAB (crude AuNRs) and dispersed in a neutral C18N3 solution. Although the AuNPs were polydisperse in shape and size, the shape homogenization of the as-synthesized AuNRs represented a level of homogeneity of approximately 90% (by number concentration). The AuNRs formed had an aspect ratio of approximately 19 and an average diameter of 18.7 nm (Figure 1a and Figure S1 in the Supporting Information). Figure 1b shows crude AuNRs dispersed by C18N3 in a neutral medium at pH 8 and then aggregated in an alkaline medium at pH 11. Perfect separation of the AuNRs from other shapes could be observed when the aggregates were redispersed in a neutral C18N3 solution at pH 8.

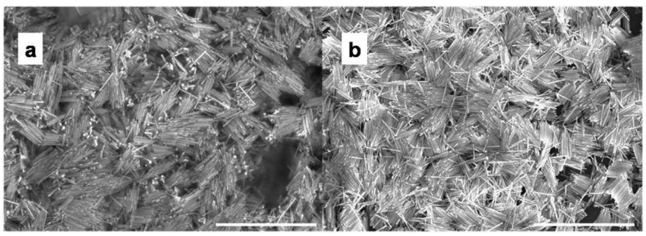

Figure 1. SEM micrographs of AuNRs deposited on silicon substrates after several washing steps with centrifugation: (a) as-synthesized crude AuNRs dispersed in a neutral CTAB solution; (b) purified AuNRs obtained by incubation with C18N3 at different pH's and then redispersed in a neutral C18N3 solution. The scale bar is 2 μm.

To understand the mechanism of this phenomenon, the solvation of different surfactants and their stabilization of AuNRs at different pH's was studied. Figure 2 shows that, in neutral water, the ability of C18N3 to deaggregate particles was much higher than that of CTAB. When an equivalent volume of highly concentrated CTAB (0.1 M) was added to AuNP aggregates, only some of the aggregates redispersed, whereas most of the large aggregates remained at the bottom of the solution (Figure 2b). However, when a neutral C18N3 solution was the dispersive medium, the NP aggregates easily redispersed, even at a concentration of C18N3 as low as 0.001 M (Figure 2c). According to the previous studies concerning the competitive adsorption between CTAB and other species,[29−31] the adsorbed CTAB could not be completely removed from the AuNR surface without using sulfur-containing compounds. However, the results reported here indicate that most of CTAB on the AuNRs is replaced by C18N3. We attributed the strong adsorption and repulsive behavior of C18N3 to its multiple amine head groups and protonated as well as deprotonated properties at different pH's. The replacement of C18N3 and formation of a double layer are possible explanations for the mechanism of shape homogenization and arrangement of AuNRs in suspension.

Although there was a significant difference in the ability of CTAB and C18N3 to deaggregate AuNPs, the sedimentation speed for AuNPs was nearly the same in both CTAB and C18N3, as shown in Figure 1a, which contained small amounts of differently shaped AuNPs. This phenomenon implies that the difference in sedimentation rates between different shapes of AuNPs is too small to separate them in the neutral medium. To increase the difference in sedimentation rates, the pH-responsive property of C18N3 was utilized. It is reported[20,21] that C18N3 not only could form stable, positively charged micelles at low pH because of protonation of its amine groups but also could be completely deprotonated at the amine functionalities at high pH, thereby causing assembly. Changing the pH of the C18N3 solution could modulate the aggregation of AuNRs. As shown in Scheme 1, crude AuNPs were

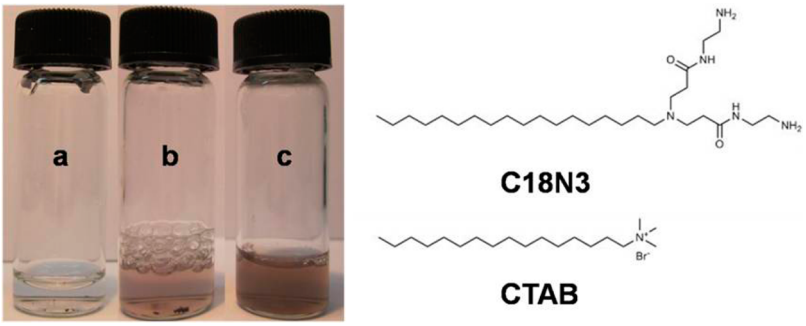

Figure 2. Comparison of the deaggregation effect of CTAB and C18N3 on crude AuNR aggregates in a neutral aqueous solution: (a) crude AuNR aggregates dispersed in a neutral aqueous solution; (b) crude AuNR aggregates redispersed in 0.1 M CTAB; (c) crude AuNR aggregates redispersed in 0.001 M C18N3.

Scheme 1. Schematic of the pH-Triggered Purification of Anisotropic AuNRs from Isotropic AuNPs Using C18N3[a]

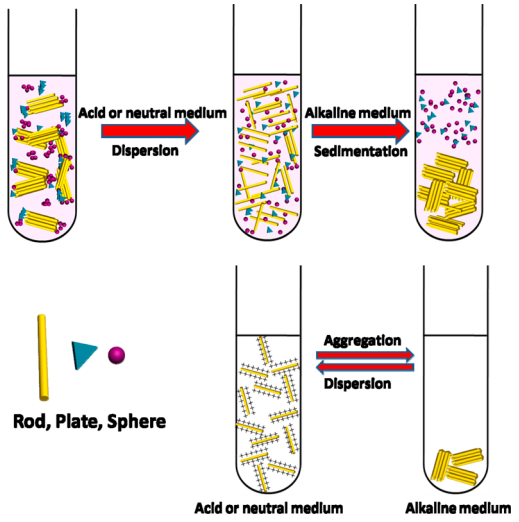

[a]Separation is based on the relative differences in the stability of the solution based on the shape.

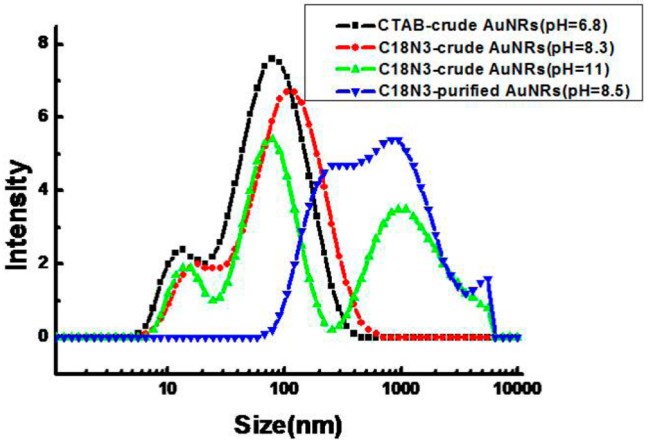

Figure 3. DLS curves of CTAB−crude AuNR dispersions at pH 6.8 (black curve), C18N3−crude AuNR at pH 8.3 (red curve), C18N3−crude AuNR at pH 11 (green curve), and purified AuNR aggregates in 0.001 M aqueous C18N3 at pH 8.5 (blue curve).

deaggregated at low pH and then aggregated at high pH. In contrast to other AuNPs with similar diameters (or widths) and minimally contacting convex surface areas, high-aspect-ratio AuNRs, which can be regarded as elongated polyhedra,[32] offer a much larger, lateral surface area that is capable of contact in a side-by-side mode, thereby resulting in a stronger tendency to aggregate than smaller, symmetrical AuNPs. Therefore, fast and more powerful separation of AuNRs can be achieved in solution.

Dynamic Light Scattering (DLS) Measurements. To gain insight into the homogenization process of AuNRs in solution, DLS measurements were performed. Figure 3 shows that crude AuNRs that were not separated by centrifugation in a neutral medium (CTAB−crude AuNRs, pH 6.8) exhibited two dispersive bands positioned at 90 and 12 nm, which characterized the AuNRs.[33,34] Moreover, the wider bands also indicated the existence of species with different shapes in solution. This result is consistent with Figure 1a, in which there are differently shaped AuNPs besides AuNRs. After rinsing and removal of the majority of CTAB by centrifugation, we added appropriate C18N3 to disperse the centrifugate, resulting in a working solution with a C18N3 concentration of approximately 0.001 M at pH 8.3 (C18N3−crude AuNRs, pH 8.3). In this case, two intensive bands, which were positioned at 120 and 18 nm, appeared in the spectrum of the solution and indicated that, by adsorption of the C18N3 molecules, the sizes of the AuNPs became larger. However, these two peaks also appeared in the spectrum of the CTAB−crude AuNRs in a neutral medium, which indicated that discrimination between sedimentation rates of differently shaped particles was still too low to separate those shapes. When the pH of the C18N3 dispersion medium was adjusted from approximately 8.3 to 11 (denoted as C18N3−crude AuNRs, pH 11, in Figure 3), a band at approximately 1000 nm arose, symbolizing the onset of aggregation for high-aspect-ratio AuNRs, which resulted from the deprotonation of C18N3, thus causing sedimentation. This step not only greatly increased the difference in the sedimentation rates between the aggregated AuNRs and the other species with different morphologies but also was essential for purification of the AuNRs. When precipitates of AuNR aggregates in solution (C18N3−crude AuNRs, pH 11) were separated and then redispersed in a 0.001 M C18N3 solution at pH 8.5 (C18N3−purified AuNRs, pH 8.5), an intense broad band appeared at approximately 1000 nm, which represented the aggregation of high-aspect-ratio AuNRs and the absence of differently shaped AuNPs. This result is consistent with observations made via SEM (Figure 1b).

Formation of a Large-Scale Arrangement of AuNRs by Using C18N3 in an Acidic Medium as the Dispersant. Figure 4 shows the arrangement of AuNRs obtained by spreading a dispersion of purified AuNRs onto silicon

dx.doi.org/10.1021/am302507u | ACS Appl. Mater. Interfaces 2012, 4, 6560−6564

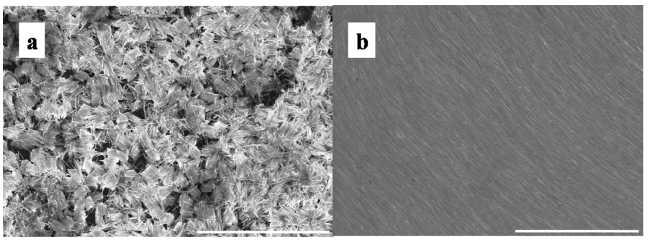

Figure 4. SEM micrographs of purified AuNRs deposited on silicon substrates following dispersion in neutral (a) and acid (b) media containing C18N3. The scale bar is 5 μm.

substrates followed by evaporation at 24 °C. Figure 4a shows that a high yield of purified AuNRs was obtained by mediating the pH of the C18N3 solution; however, a long-range ordered arrangement of high-aspect-ratio AuNRs was not achieved. On the basis of the mechanism mentioned above, a 0.001 M C18N3 solution at pH 4 was substituted for the neutral C18N3 solution as the redispersion medium. Interestingly, a beautiful, large region of ordered high-aspect-ratio AuNRs with an area of several dozens of square micrometers (Figure 4b) was obtained. However, when using a 0.001 M C18N3 solution at pH 8 as the dispersion medium, only smaller ordered domains were achieved, as shown in Figure 4a. We attributed this phenomenon to the presence of a thick double layer of C18N3 at low pH, which decreases the speed of aggregation of AuNRs and allows more time for the entropy-driven self-arrangement of AuNRs.[35−37]

Optical Absorption Spectrum of High-Aspect-Ratio Purified AuNPs. It is widely accepted that the absorption spectrum can mirror the presence of AuNPs with different geometries.[38] Figure 5 compares the absorption spectra of crude AuNRs and purified AuNRs dispersed in a C18N3 solution. The surface plasmon absorption spectrum for the crude AuNRs has two bands: a strong band at long wavelength from the longitudinal oscillation of electrons and a weak band at short wavelength of approximately 520 nm from the transverse oscillation of electrons. The intense absorption band at around 520−540 nm is due to the presence of gold nanospheres and transverse absorption of the targeted product AuNRs.[39,40] Moreover, the band centered from 910 to 1000 nm that is attributed to the total light absorption of in-plane quadrupole and in-plane dipole mode resonances of the triangular and truncated triangular nanoplates[41] is also observed (black curve in Figure 5). After shape homogenization, the absorption band at around 520−540 nm becomes much weaker (red curve in Figure 5a), which is due to the removal of the isotropic AuNPs. The absence of the absorption band in the range of 800−1000 nm indicates that the amounts of triangular and truncated triangular nanoplates are very minimal while the intensity of the longitudinal surface plasmon resonance band is still very strong (red curve in Figure 5b). The intense adsorption of the purified high-aspect-ratio AuNRs in the NIR region (Figure 5b) is quite important for applications in optical and medical devices.

4. CONCLUSIONS

In summary, we have developed a new convenient, time-saving, and scalable technique to successfully purify high-aspect-ratio, NIR-responsive AuNRs from crude AuNRs with a purity of approximately 99% by the number density. These purified AuNRs were used to form a large ordered domain of high-aspect-ratio AuNRs with an area of up to several dozens of square micrometers on a silicon substrate and demonstrated an interesting narrowing effect on the spectral bands in the extinction spectra in the NIR region. The crux of our strategy lies in the use of a surfactant with multiple amine heads as a surface modifier, which protonates and disperses AuNPs in both acidic and neutral aqueous media but which deprotonates and precipitates these particles in an alkaline medium. It is expected that the purification and arrangement methods used here can be applied to other anisotropic NP systems. Because C18N3 is only one member of the multiamine surfactant family, a new application area has been opened for multiamine surfactants with respect to the fabrication and arrangement of several nanostructures. Furthermore, the arrangement of a large area of NIR-responsive AuNRs obtained here is important for future applications in molecular sensing, nanostructure integration, and advanced optical and medical nanodevices.

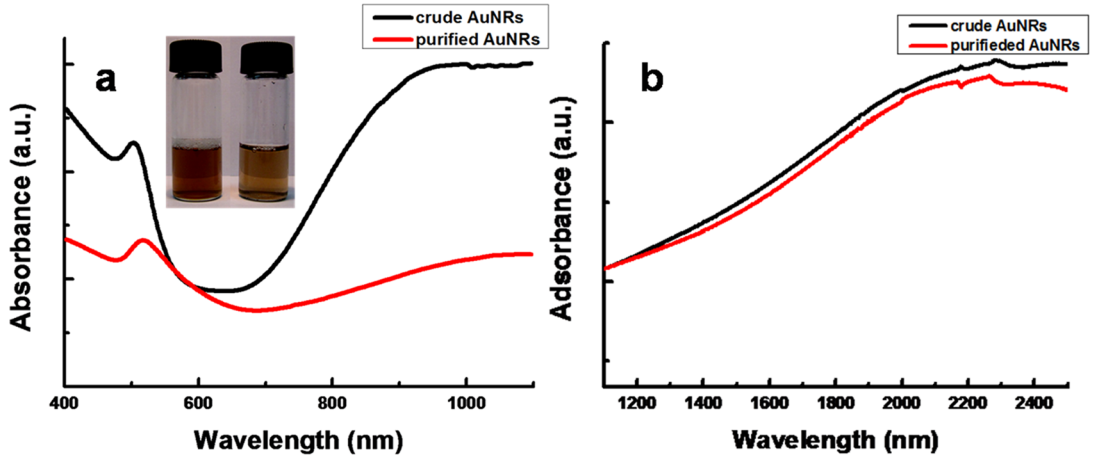

Figure 5. (a) Normalized UV−vis absorbance spectra of crude (black curve) and purified (red curve) AuNRs dispersed in aqueous solution. (b) Absorbance spectra of crude (black curve) and purified (red curve) AuNRs that are deposited onto a quartz substrate and then dried. The photograph (inset) in part a shows the corresponding dispersions of crude and purified AuNRs from left to right.

■ ASSOCIATED CONTENT

Supporting Information

SEM images, a distribution histogram, and a TEM image of AuNRs. This material is available free of charge via the Internet at http://pubs.acs.org.

■ AUTHOR INFORMATION

Corresponding Author

*E-mail: jiangl@iccas.ac.cn (L.J.), luwensheng@iccas.ac.cn (W.L.).

Notes

The authors declare no competing financial interest.

■ ACKNOWLEDGMENTS

This research is supported by the National Natural Science Foundation of China (Grants 20933007, 20903106, 21021003, 91127012, and 21161130512).

■ REFERENCES

(1) Lianke, L.; Zhirui, G.; Lina, X.; Ruizhi, X.; Xiang, L. *Nanoscale Res. Lett.* **2011**, *6*, 143−148.
(2) Sau, T. K.; Rogach, A. L.; Jäckel, F.; Klar, T. A.; Feldmann, J. *Adv. Mater.* **2010**, *22* (16), 1805−1825.
(3) Xia, Y.; Xiong, Y.; Lim, B.; Skrabalak, S. E. *Angew. Chem., Int. Ed.* **2009**, *48* (1), 60−103.
(4) Murphy, C. J.; Gole, A. M.; Hunyadi, S. E.; Stone, J. W.; Sisco, P. N.; Alkilany, A.; Kinard, B. E.; Hankins, P. *Chem. Commun.* **2008**, *5*, 544−557.
(5) Gao, J.; Bender, C. M.; Murphy, C. J. *Langmuir* **2003**, *19* (21), 9065−9070.
(6) El Khoury, J. M.; Zhou, X.; Qu, L.; Dai, L.; Urbas, A.; Li, Q. *Chem. Commun.* **2009**, No. 16, 2109−2111.
(7) Li, Y.; Yu, D.; Dai, L.; Urbas, A.; Li, Q. *Langmuir* **2011**, *27* (1), 98−103.
(8) Xue, C.; Birel, O.; Gao, M.; Zhang, S.; Dai, L.; Urbas, A.; Li, Q. *J. Phys. Chem. C* **2012**, *116* (18), 10396−10404.
(9) Burda, C.; Chen, X.; Narayanan, R.; El-Sayed, M. A. *Chem. Rev.* **2005**, *105* (4), 1025−1102.
(10) Murray, C.; Norris, D.; Bawendi, M. G. *J. Am. Chem. Soc.* **1993**, *115* (19), 8706−8715.
(11) Nikoobakht, B.; El-Sayed, M. A. *Chem. Mater.* **2003**, *15* (10), 1957−1962.
(12) Pérez-Juste, J.; Pastoriza-Santos, I.; Liz-Marzán, L. M.; Mulvaney, P. *Coord. Chem. Rev.* **2005**, *249* (17), 1870−1901.
(13) Zheng, Y.; Lalander, C. H.; Bach, U. *Chem. Commun.* **2010**, *46* (42), 7963−7965.
(14) Guo, Z.; Fan, X.; Xu, L.; Lu, X.; Gu, C.; Bian, Z.; Gu, N.; Zhang, J.; Yang, D. *Chem. Commun.* **2011**, *47* (14), 4180−4182.
(15) Khanal, B. P.; Zubarev, E. R. *J. Am. Chem. Soc.* **2008**, *130* (38), 12634−12635.
(16) Kowalczyk, B.; Lagzi, I.; Grzybowski, B. A. *Curr. Opin. Colloid Interface Sci.* **2011**, *16*, 135−148.
(17) Sharma, V.; Park, K.; Srinivasarao, M. *Proc. Natl. Acad. Sci. U.S.A.* **2009**, *106* (13), 4981−4985.
(18) Hamon, C.; Postic, M.; Mazari, E.; Bizien, T.; Dupuis, C.; Even-Hernandez, P.; Jimenez, A.; Courbin, L.; Gosse, C.; Artzner, F. *ACS Nano* **2012**, *6* (5), 4137.
(19) Ng, K. C.; Udagedara, I. B.; Rukhlenko, I. D.; Chen, Y.; Tang, Y.; Premaratne, M.; Cheng, W. *ACS Nano* **2012**, *6*, 925−934.
(20) Jia, W.; Li, J.; Lin, G.; Jiang, L. *Cryst. Growth Des.* **2011**, *11* (9), 3822−3827.
(21) Wang, W.; Lu, W.; Jiang, L. *J. Phys. Chem. B* **2008**, *112* (5), 1409−1413.
(22) Tao, A.; Kim, F.; Hess, C.; Goldberger, J.; He, R.; Sun, Y.; Xia, Y.; Yang, P. *Nano Lett.* **2003**, *3* (9), 1229−1233.
(23) Guerrero-Martínez, A.; Pérez-Juste, J.; Carbó-Argibay, E.; Tardajos, G.; Liz-Marzán, L. M. *Angew. Chem., Int. Ed.* **2009**, *48* (50), 9484−9488.
(24) Park, H. S.; Agarwal, A.; Kotov, N. A.; Lavrentovich, O. D. *Langmuir* **2008**, *24* (24), 13833−13837.
(25) Xie, Y.; Guo, S.; Ji, Y.; Guo, C. F.; Liu, X.; Chen, Z.; Wu, X.; Liu, Q. *Langmuir* **2011**, *27*, 11394−11400.
(26) Hu, X.; Cheng, W.; Wang, T.; Wang, E.; Dong, S. *Nanotechnology* **2005**, *16*, 2164−2169.
(27) Lereu, A.; Passian, A.; Farahi, R.; Abel-Tiberini, L.; Tetard, L.; Thundat, T. *Nanotechnology* **2012**, *23*, 045701−045713.
(28) Wu, H. Y.; Huang, W. L.; Huang, M. H. *Cryst. Growth Des.* **2007**, *7* (4), 831−835.
(29) Lee, S.; Anderson, L. J. E.; Payne, C. M.; Hafner, J. H. *Langmuir* **2011**, *27* (24), 14748−14756.
(30) Khanal, B. P.; Zubarev, E. R. *Angew. Chem., Int. Ed.* **2007**, *46* (13), 2195−2198.
(31) Vigderman, L.; Manna, P.; Zubarev, E. R. *Angew. Chem., Int. Ed.* **2012**, *124* (3), 660−665.
(32) Smith, D. K.; Miller, N. R.; Korgel, B. A. *Langmuir* **2009**, *25* (16), 9518−9524.
(33) Pan, B.; Cui, D.; Xu, P.; Li, Q.; Huang, T.; He, R.; Gao, F. *Colloids Surf., A* **2007**, *295* (1-3), 217−222.
(34) Lee, S. E.; Sasaki, D. Y.; Perroud, T. D.; Yoo, D.; Patel, K. D.; Lee, L. P. *J. Am. Chem. Soc.* **2009**, *131* (39), 14066−14074.
(35) Jana, N. R. *Chem. Commun.* **2003**, *15*, 1950−1951.
(36) Ha, T. H.; Kim, Y. J.; Park, S. H. *Chem. Commun.* **2010**, *46* (18), 3164−3166.
(37) Park, K.; Koerner, H.; Vaia, R. A. *Nano Lett.* **2010**, *10* (4), 1433−1439.
(38) Liz-Marzán, L. M. *Langmuir* **2006**, *22* (1), 32−41.
(39) Huang, X.; El-Sayed, I. H.; Qian, W.; El-Sayed, M. A. *J. Am. Chem. Soc.* **2006**, *128*, 2115−2120.
(40) Burda, C.; Chen, X .; Narayanan, R.; El-Sayed, M. A. *Chem. Rev.* **2005**, *105* (4), 1025−1102.
(41) Ah, C. S.; Yun, Y. J.; Park, H. J.; Kim, W. J.; Ha, D. H.; Yun, W. S. *Chem. Mater.* **2005**, *17* (22), 5558−5561.